Chapter

UWB-MIMO Antenna with Band-Notched Characteristics for Portable Wireless Systems

Chandrasekhar Rao Jetti and
Venkateswara Rao Nandanavanam

Abstract

The current and future wireless communication systems demand for higher data rates, enhanced quality of service and more channel capacity. Since Federal Communications Commission (FCC) allocated the unlicensed frequency spectrum from 3.1 to 10.6 GHz for commercial applications in the year 2002, Ultra-Wideband (UWB) technology has attained considerable attention because of its inherent features like high data rate, more channel capacity, extremely less power consumption and low cost. However, for UWB systems, multipath fading and frequency interference are the two significant issues that requires further investigation. In recent times, Multiple Input Multiple Output (MIMO) technology has gained much attention in wireless communication as it exploits multipath to increase the communication range and link quality. Thus, MIMO technology is a promising solution for mitigating multipath fading in UWB system. However, accommodating multiple antennas with less mutual coupling between them in portable devices is always a challenging task for antenna designers. UWB system could easily interfere with existing narrowband communication system such as Wireless Local Area Network (WLAN). So, the design of an ultra-wideband antenna with integrated frequency notching function is a good solution to suppress the frequency interference and to reduce the complexity of the UWB system instead of using a conventional filter. In this chapter, compact isolation-enhanced planar UWB-MIMO antenna with single band-notched characteristics is presented.

Keywords: ultra-wideband, multipath fading, frequency interference, multiple input multiple output, mutual coupling, isolation, band-notch

1. Introduction

The primary concerns of wireless communication systems are higher data rates, improved quality of service, more channel capacity, low power consumption and less interference with other systems. Ultra Wideband technology is the most promising technology to meet the requirements of wireless communication system because of its advantages, such as higher data rate transmission, low cost, high security, and less power requirement [1]. However, multipath fading and frequency interference with other communication systems are the important problems should be well solved for UWB systems.

In an indoor communication application, like other wireless communication systems, the UWB system performance is also restricted by multipath fading due to rich scattering environments which cause inter-symbol interference. In present times, digital communication using multiple input multiple output (MIMO) technology has emerged as a breakthrough for a wireless system. The MIMO system employs multiple antennas at the transmitter and receiver. It makes use of the rich multipath environment to mitigate the multipath fading effect. And it improves the range of communication and system capacity (data rate) without the need for additional bandwidth or transmitted signal power [2, 3]. Hence, the UWB system with MIMO technology is a viable solution to reduce the multipath fading effect and to improve the quality of service, the range of communication and system capacity [4].

The electromagnetic interaction between the radiating (antenna) elements in multiple antenna or MIMO system is known as mutual coupling. The closely spaced antennas, especially in portable devices, inevitably cause strong mutual coupling between antennas. The mutual coupling is undesirable which causes fluctuations in the input impedance of individual antenna element i.e., impedance mismatch which degrades the radiation efficiency, deviations in antenna radiation pattern due to the high correlation between antenna signals and decreases the channel capacity of MIMO system. Since the mutual coupling has a considerable impact on the MIMO system performance, the reduction of mutual coupling between antennas and enhancement of isolation between ports is imperative. However, placing multiple antennas in a space-limited portable wireless device is a big challenge for antenna designers [5]. Hence, designing compact UWB-MIMO antenna exhibiting band-notch function and less mutual coupling is very much needed. Various designs were proposed in the recent years to suppress the effects of mutual coupling in ultra-wideband MIMO antennas [6–15]. Methods include, placing radiating elements perpendicular to each other and adding two long protruding stubs to ground [6], use of tree-like structure on the ground plane [7], etching a T-shaped slot and a line slot on the ground [8], adding a Y-shaped slot on the T-shaped protruded ground plane [9], placing two shorts at 45 degrees between the microstrip lines and in the opposite direction [10], protruding ground structure [11], T-shaped metallic stub [12, 13], adopting wideband neutralization line [14] and using modified ground structure along with T-shaped slot on the ground [15].

Ultra-wideband is an emerging technology for short distance low power communications. It makes use of short duration pulses which have very low power spectral density for transmission of data. Since the UWB system is operating from 3.1 to 10.6 GHz, it could easily interfere with existing narrowband communication system like Wireless Local Area Network (WLAN-5.15–5.825 GHz). So, ultra-wideband antenna with integrated frequency notching function at the interfering frequency band is a feasible solution to mitigate the frequency interference [16]. The power spectral density of UWB and other narrowband systems is shown in **Figure 1**. The frequency interference produced by a UWB transmitter to a narrowband system is very negligible because of the transmitted signal emission power (power spectral density) is very less compared with narrowband systems. But, when a UWB receiver is located very near to the narrowband interferer, the interference caused is very high. So, a notch at the interfering frequency is needed to suppress its effect. The traditional RF filter circuits using lumped elements can be used to implement this frequency notching feature but, it increases the system complexity, cost and occupies more space when integrated with other microwave circuits in the portable device. Another viable solution is to design a UWB antenna with an integrated band-notched feature to mitigate the frequency interference which decreases the complexity and cost of the UWB system. The idea of designing

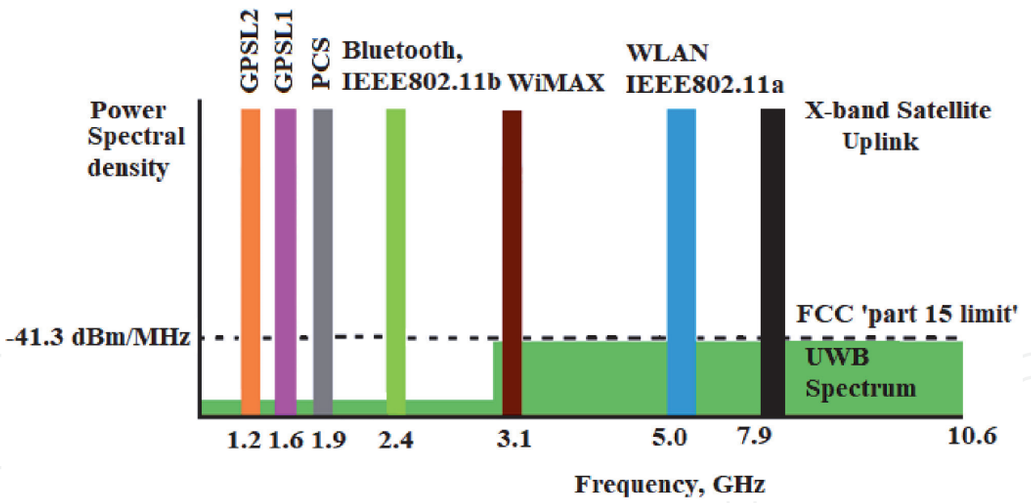

Figure 1.
The power spectral density of UWB and other narrowband systems.

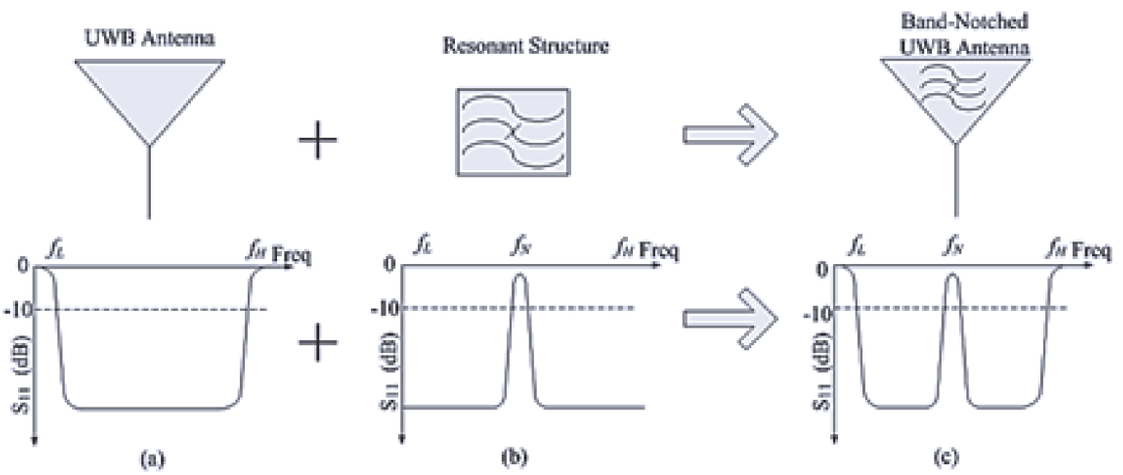

Figure 2.
The basic design of UWB antenna with band-notched characteristic: (a) UWB antenna, (b) Band-notch resonant structure and (c) Band-notched UWB-antenna.

the UWB antenna with band-notched characteristic is shown in **Figure 2** [17, 18]. The basic UWB antenna is having impedance bandwidth from [f_L-f_H] as shown in **Figure 2(a)**, where f_L and f_H are the lowest and highest −10 dB cut-off frequencies of S_{11}, respectively. A band-stop resonant structure also has the impedance bandwidth from [f_L-f_H], but with notch (resonant) frequency at f_N to stop the unwanted frequencies as shown in **Figure 2(b)**. The UWB antenna combining with a band-stop resonant circuit forms band-notched UWB antenna is shown in **Figure 2(c)**. The band-notched UWB antenna does not interfere with existing communication systems which are operating at f_N. Hence, the design of UWB antennas with band-notched function is needed.

The band-notch characteristics for UWB systems can be obtained by integrating band-notch resonator (like slots, split ring resonators, strips and stubs) to the UWB antenna. The possible locations for integration of band-notch resonator are: on or adjacent to radiator or feed line or on the ground as given in **Figure 3**. The length of the band-notch resonator controls the notch center frequency. However, the desired notch band is obtained by proper tuning of length and width of the resonator. The total length of the band-notch resonator should be λ/2 or λ/4 corresponding to the notched-band center frequency as given in equations (1) and (2) [19], where λ is the guided wavelength.

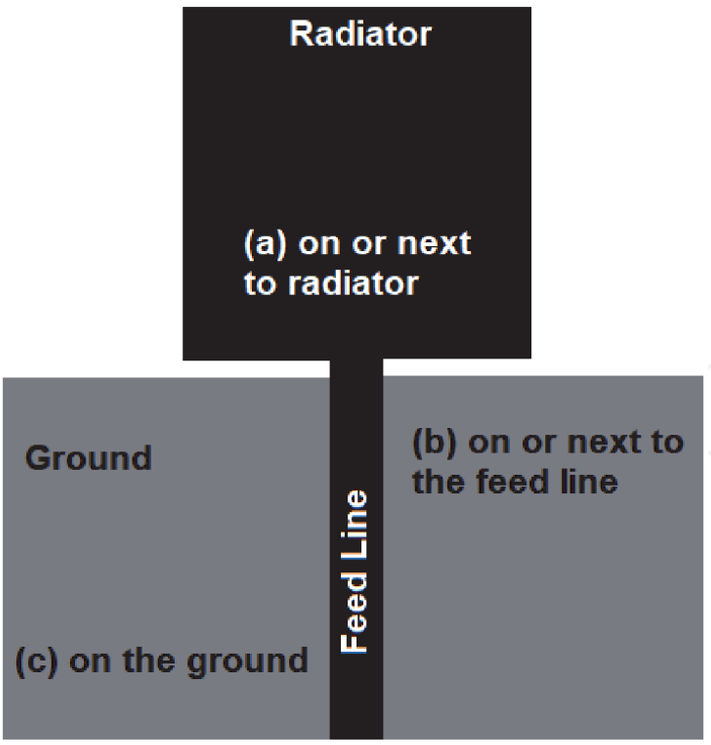

Figure 3.
Possible locations of resonant structure on UWB antenna.

$$L_{Notch} = \frac{c}{2f_{Notch}\sqrt{\varepsilon_{eff}}}, \tag{1}$$

or

$$L_{Notch} = \frac{c}{4f_{Notch}\sqrt{\varepsilon_{eff}}}, \tag{2}$$

$$\lambda = \frac{c}{f_{Notch}\sqrt{\varepsilon_{eff}}}, \tag{3}$$

$$\varepsilon_{eff} = \frac{(1+\varepsilon_r)}{2}, \tag{4}$$

where c denotes light speed, f_{Notch} represents notch center frequency, L_{Notch} is the total length of slot or strip, ε_{eff} indicates effective dielectric constant and ε_r denotes dielectric constant.

Several investigations were reported earlier to create band notch function at WLAN band for ultra-wideband systems in [19–30]. Methods include inserting λ/4 and λ/2 slot resonators on the ground plane [19], using a pair of ground stubs locating along the edge of the ground plane [20], inserting open stub in the printed folded monopole [21], etching folded U-shaped slots in the feed line of the antenna [22, 23], incorporating SRR slots on radiating element [24], quarter-wave stub connected to the ground [25], adding protruding two rectangular stubs on the ground plane [26], with a slot of length 1.0 λ in the radiator [27], open-ended quarter-wavelength L-shaped slots were etched on the rectangular radiating patches [28], using C-shaped and Z-shaped slot resonators on the ground [29], employing elliptical SRR on the radiating element [30].

The antenna designs presented in the above literature exhibiting acceptable isolation and notching characteristics, but some designs were not compact enough and few are a bit complex. So, the design of simple and compact band-notched

ultra-wideband MIMO antenna with low mutual coupling is needed. In this chapter, we have presented compact isolation-enhanced planar UWB-MIMO antenna with single band-notched characteristics at WLAN band [31]. Ansoft HFSS v.13 is used to carry out the proposed antenna design, optimization, and simulations. For validating the simulation results, all the proposed antenna has been fabricated and tested using the Agilent N5224A PNA, Anritsu MS2037C vector network analyzer and an anechoic chamber. In Section 2, UWB-MIMO antenna with single band-notched characteristic is discussed. Finally, conclusions of the work are given in Section 3.

2. UWB-MIMO antenna with single band-notched characteristic

Compact ultra-wideband MIMO antenna exhibiting band-notch characteristics at WLAN band (5 to 5.9 GHz) for portable wireless devices is presented in this section [31]. The following sub sections discusses the detailed description of the proposed design.

2.1 Antenna design

The geometry of the proposed single band-notch UWB-MIMO antenna and photograph of the fabricated antenna are shown in **Figure 4(a)** and **(b)**. The design is printed on an FR4 substrate having dielectric constant (ε_r) of 4.4, a thickness of 0.8 mm, and a loss tangent of 0.02. The overall size of the proposed antenna is L $\times$ W $\times$ h mm^3 = 26 $\times$ 40 $\times$ 0.8 mm^3. The antenna comprises two identical rectangular planar monopole radiating elements, denoted as PM1 and PM2 having sizes L_R $\times$ W_R as shown in **Figure 4(a)**. Both PM1 and PM2 are fed by the 50-ohm coplanar waveguide having dimensions F_{L1} $\times$ W_F. And, the common ground is formed by joining L_G $\times$ W_G and L_G $\times$ L reduced ground planes and is also printed on the same side of the substrate. The planar monopoles PM1 and PM2 are positioned perpendicularly to each other to reduce the mutual coupling between the elements and to improve the isolation between the antenna ports. A long rectangular strip of size S_L $\times$ S_W is extended from the common ground plane between the monopoles to further enhance isolation and improve the impedance bandwidth of the antenna. The ground strip extends the current path which shifts the first resonance frequency to lower band and blocks the surface currents to minimizes the mutual coupling. An inverted U-slot resonator is placed on the feed line to create a band-notch function at 5–5.9 GHz. The antenna optimized dimensions are given as follows: (unit: mm): D_1 = 5.1, D_2 = 6.1, D_3 = 11.2, F_{L1} = 9.5, F_{L2} = 1.5, F_{L3} = 0.4, L = 26, L_G = 8, L_R = 10, S_L = 18, S_W = 1, W = 40, W_F = 1.8, W_G = 3.2, W_R = 11, U_1 = 7.8, U_2 = 0.4, and U_W = 0.3. **Figure 5(a)** and **(b)** shows the simulated *S*-parameters such as S_{11} and S_{21} of the Antenna 1 (UWB-MIMO antenna without ground strip), Antenna 2 (UWB-MIMO with a ground strip), and the proposed antenna. It can be observed that the proposed ultra-wideband MIMO antenna is operating from 2.2 to 11.4 GHz with good impedance bandwidth except at notch band from 5 to 5.9 GHz. Also, the mutual coupling of less than −20 dB is obtained over the entire UWB band.

2.2 Study of MIMO antenna

Since the ground and radiating elements are having smaller dimensions, the flow of surface currents on the ground plane and near-field radiation leads to poor impedance matching and high mutual coupling, which restricts the performance of MIMO antenna. The ultra-wideband MIMO antenna without and with ground strip

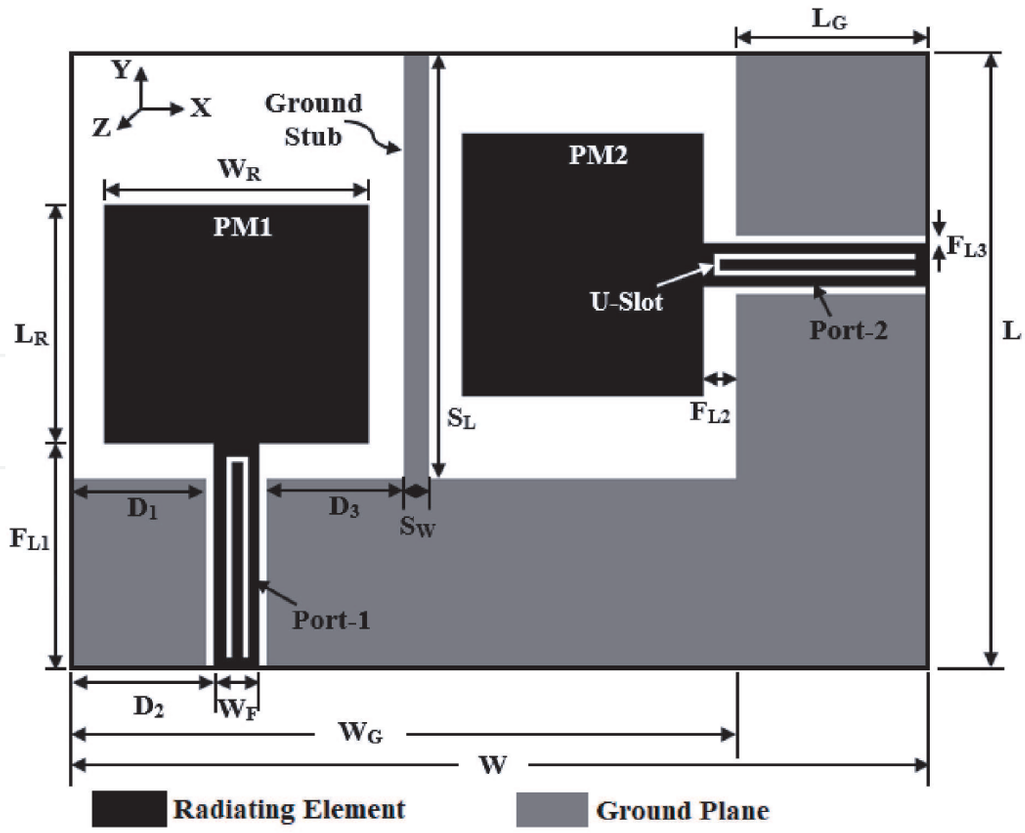

(a)

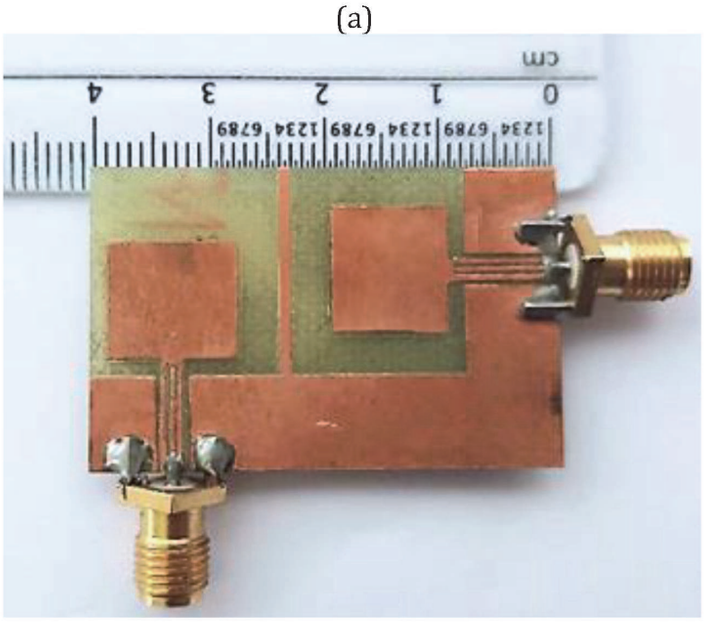

(b)

Figure 4.
(a) Geometry of the proposed antenna and (b) fabricated antenna.

is shown in **Figure 6(a)** and **(b)**, respectively. The effects of the ground strip on impedance bandwidth and mutual coupling between the MIMO antenna elements are plotted in **Figure 7(a)** and **(b)**. With ground strip between the PM1 and PM2 (Antenna 2), the first resonance is generated at 2.5 GHz with a lower cutoff frequency of 2.3 GHz and provides good impedance bandwidth from 2.3 to 11.4 GHz as depicted in **Figure 7(a)**. And, from **Figure 7(b)**, the mutual coupling of lower than −20 dB between the antenna elements is observed throughout the UWB band which is less than −17 dB. In addition, the flow of surface currents is effectively

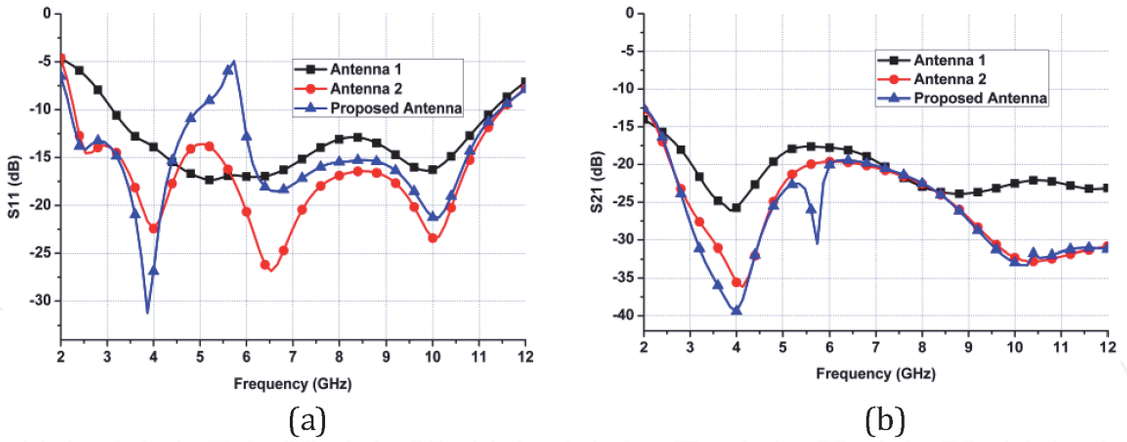

Figure 5.
Simulated S-parameters. (a) Simulated S11 parameter. (b) Simulated S21 parameter.

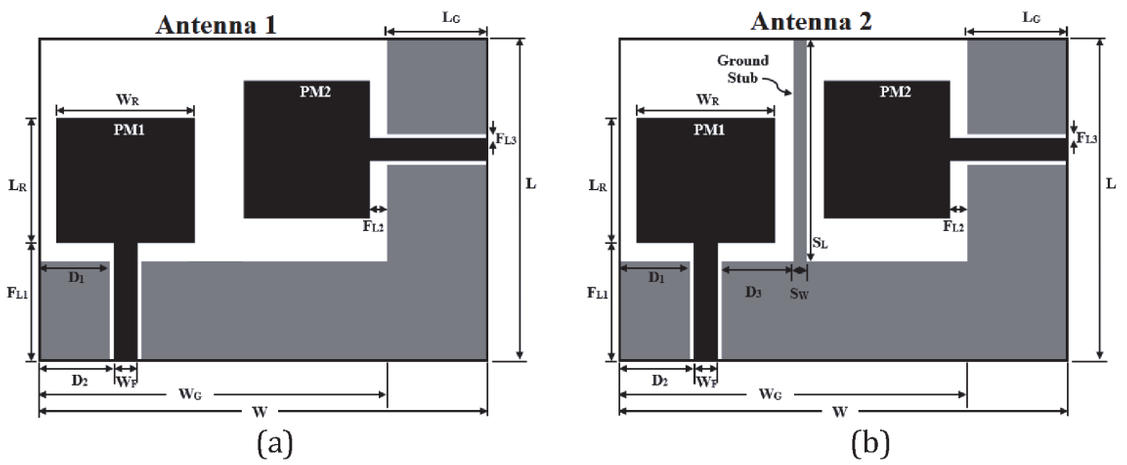

Figure 6.
(a) UWB-MIMO antenna without a ground strip (Antenna 1), (b) UWB-MIMO antenna with a ground strip (Antenna 2).

suppressed by the ground strip and thus less amount of current is leaked into the port 2 when port 1 is excited as displayed in **Figure 7(c)**. The ground strip can work as a reflecting surface so that the direction of surface currents is diverted and thus the distance between the ports is increased. Hence, the isolation between the MIMO antenna ports is significantly enhanced. Also, the ground strip between the MIMO antenna elements will improve impedance matching characteristics and minimizes the mutual coupling of the MIMO antenna. The MIMO antenna is also studied by varying the ground strip length S_L and width S_W and are plotted in **Figure 8(a)–(d)** and the same tabulated in **Table 1**. It can be observed from that the total length and width of the ground strip has more effect on the impedance bandwidth ($|S_{11}| < -10$ dB) than the isolation or mutual coupling. In this work, the ground strip length S_L = 18 mm and width S_W = 1 mm is adopted.

To create band-notch filtering function for ultra-wideband systems, slots of various shapes or split-ring resonators or strips can be used on or next to the feed line or the radiating element or the ground plane as reported earlier. The slot or SRR or strip can act as a band-notch resonator. The notch band center frequency is controlled by the length of the resonator and notch band bandwidth is controlled by the width of the resonator. In this design, an inverted U-shaped slot is used as a band-notch resonator and is etched on the feed line of Antenna 2 which forms the

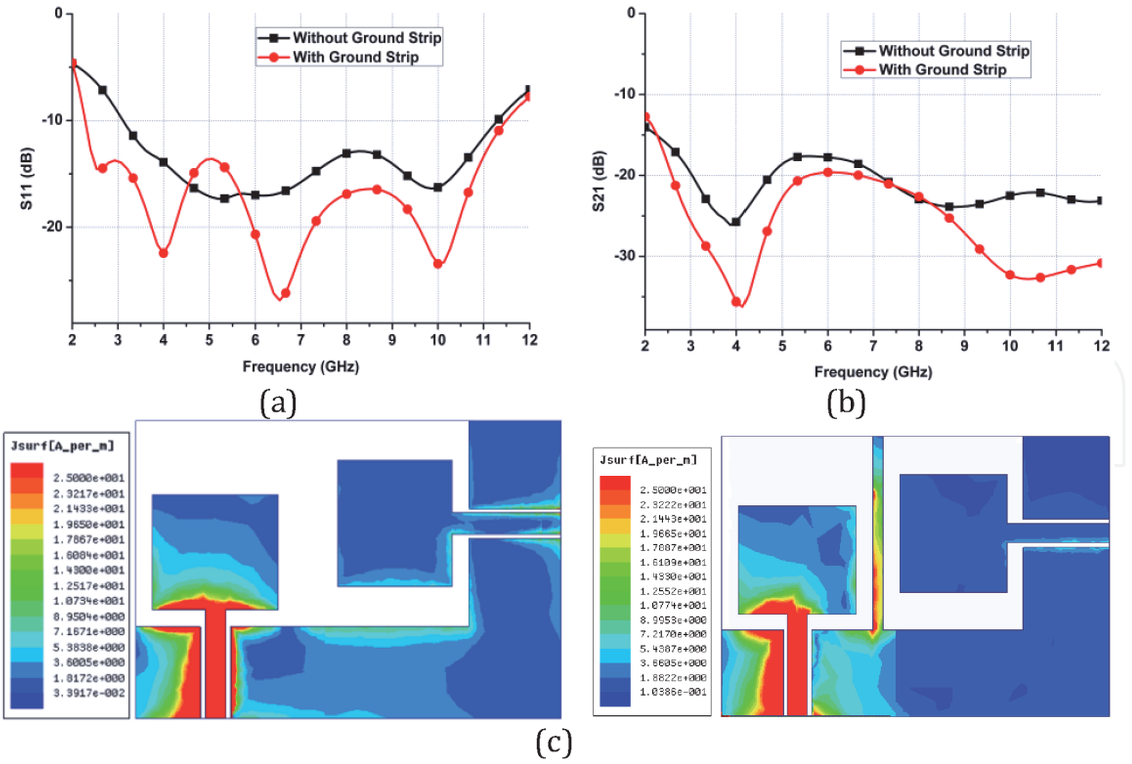

Figure 7.
(a) S11 without and with a ground strip, (b) S21 without and with a ground strip (c) surface current distribution at 3.8 GHz when port 1 excited without and with a ground strip.

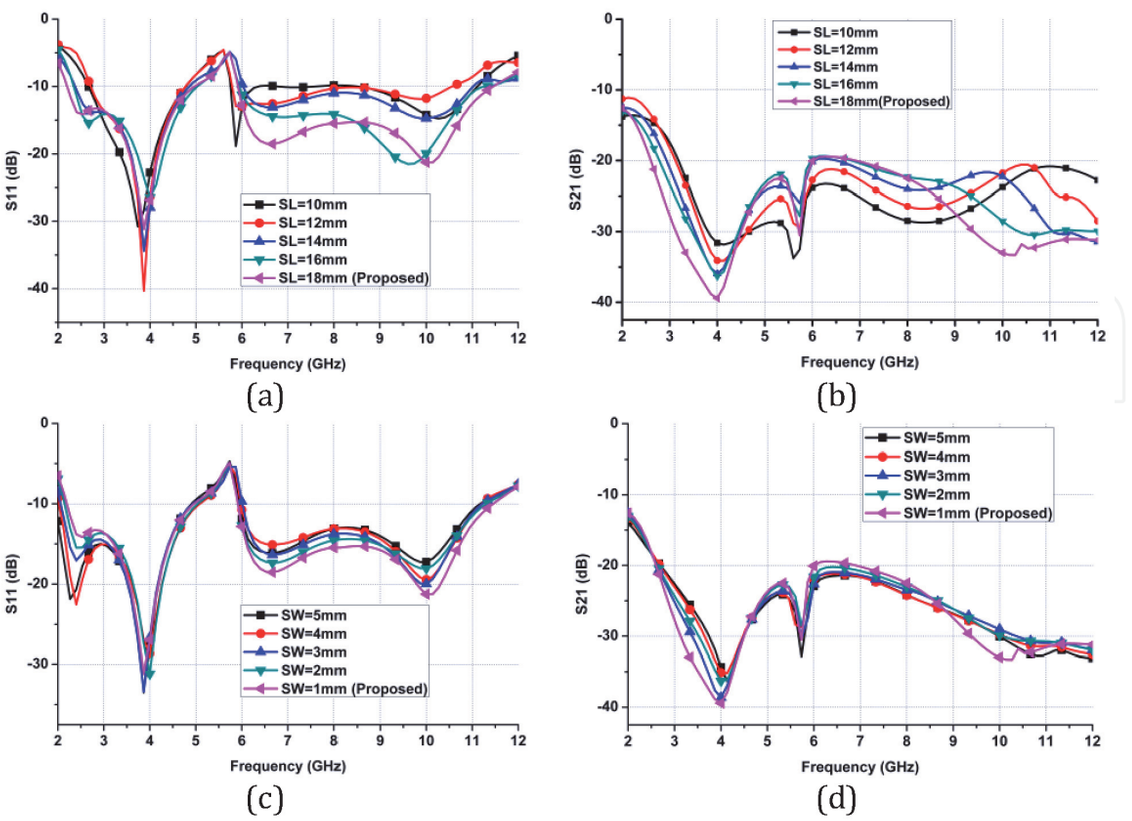

Figure 8.
(a) S11 for different strip lengths SL, (b) S21 different strip lengths SL, (c) S11 for different strip widths SW, (d) S21 for different strip widths SW.

Parameter	Value (mm)	Bandwidth (S_{11} < −10 dB)	Mutual coupling (S_{21} < −20 dB)
Strip length S_L	10	2.6–6.4	3.3–11.4
	12	2.6–8.6	3.2–11.4
	14	2.4–11.0	2.9–11.4
	16	2.4–11.3	2.8–11.4
	18 (proposed)	2.2–11.4	2.6–11.4
Strip width S_W	5	2.0–11.1	2.8–11.4
	4	2.0–11.1	2.8–11.4
	3	2.1–11.2	2.8–11.4
	2	2.2–11.2	2.7–11.4
	1 (proposed)	2.2–11.4	2.6–11.4

Table 1.
The S_{11} and S_{21} for various strip lengths and widths except at notch band.

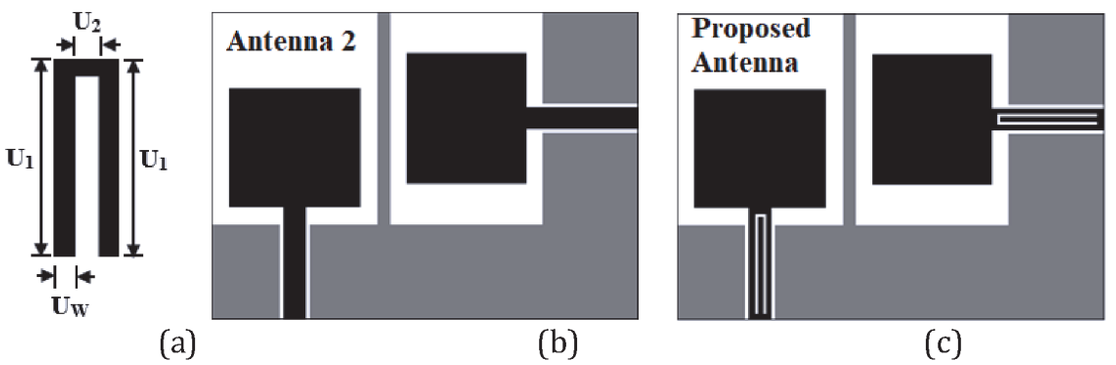

Figure 9.
(a) An inverted U-slot resonator, (b) UWB-MIMO antenna with ground strip (Antenna 2), (c) proposed band-notched UWB-MIMO antenna.

proposed band-notch UWB-MIMO antenna as shown in **Figure 9(a)–(c)**. The length of the U-shaped resonator is calculated using Eq. (5) [19]:

$$L_N = \frac{c}{2f_N\sqrt{\varepsilon_{eff}}} \approx \frac{\lambda}{2}, \tag{5}$$

where L_N denotes the total length of U-slot and f_N is notch center frequency. When f_N = 5.7 GHz and ε_r = 4.4, the calculated length of the U-slot resonator using equation (5) is 16.01 mm. The simulated or designed total length of the inverted U-slot resonator is 16 mm and is determined by using equation (6).

$$L_{U-Slot} = 2\,U_1 + U_2 \approx \frac{\lambda}{2}. \tag{6}$$

Good agreement between the calculated (theoretical) length and simulated (practical) length is observed. **Figure 10(a)–(c)** shows the S_{11}, S_{21} and surface currents without and with inverted U-slot resonator. As seen in **Figure 10(a)**, the proposed antenna is working from 2.2 to 11.4 GHz with good impedance bandwidth and generates band-notch characteristics from 5 to 5.9 GHz with S_{11} of −5 dB at 5.7 GHz. And the mutual coupling of below −20 dB over the entire working band is observed as from the **Figure 10(b)**. It is evident from **Figure 10(c)** that at 5.7 GHz,

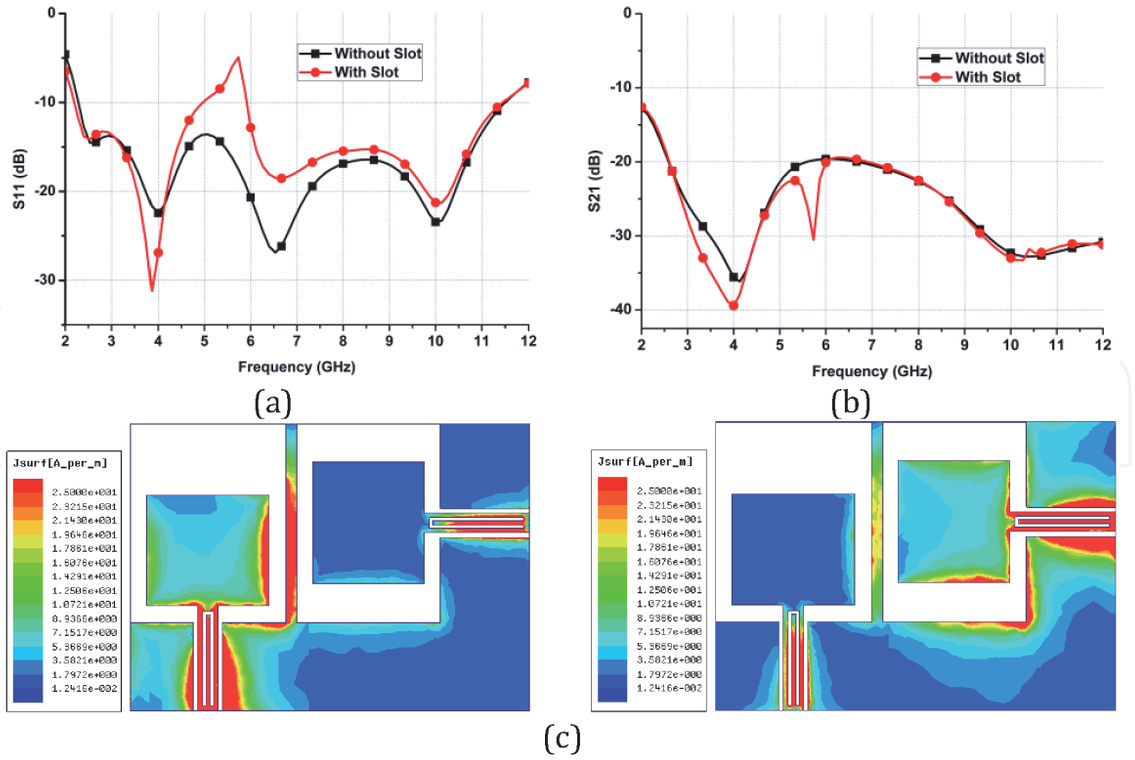

Figure 10.
(a) S11 without and with inverted U-slot, (b) S21 without and with inverted U-slot (c) current distribution at 5.7 GHz when port 1 and port 2 excited.

Parameter	Value (mm)	Notch-band (GHz)	Notch-center frequency f_N (GHz)
Slot length U_1	6.8	6.26–6.7	6.5
	7.3	5.73–6.4	6.2
	7.8 (proposed)	5.0–5.9	5.7
	8.1	4.8–5.7	5.4
Slot width U_W	0.25	5.2–5.7	5.6
	0.3 (proposed)	5.0–5.9	5.7
	0.35	4.95–6	5.7
	0.4	4.94–6.1	5.7

Table 2.
The notch bands and notch center frequencies for different slot lengths and widths.

heavy current is concentrated around the inverted U-slot resonator which acts a band-notch filter, so the current flow on the radiating elements is blocked and hence no radiation from the antenna. Therefore, notch band from 5 to 5.9 GHz WLAN band is created.

The parametric analysis on the slot length U_1 and slot width U_W is performed to describe the effects of inverted U-slot. **Table 2** shows the notch bands and notch center frequencies for different slot lengths and widths. **Figure 11(a)** and **(b)** illustrates the S_{11} of the MIMO antenna for different slot lengths U_1 and slot widths U_W, respectively. It is evident that as the slot length U_1 increasing from 6.8 mm to 8.1 mm, the center frequency of notch f_N is decreasing from 6.5 GHz to 5.4 GHz and notch band is shifting from (6.26–6.7) GHz to (4.8–5.7) GHz. The required band notch from 5 to 5.9 GHz is generated for U_1 of 7.8 mm which is used in this design. Form **Figure 11(b)**, it can be observed that increasing the slot width U_W from 0.25

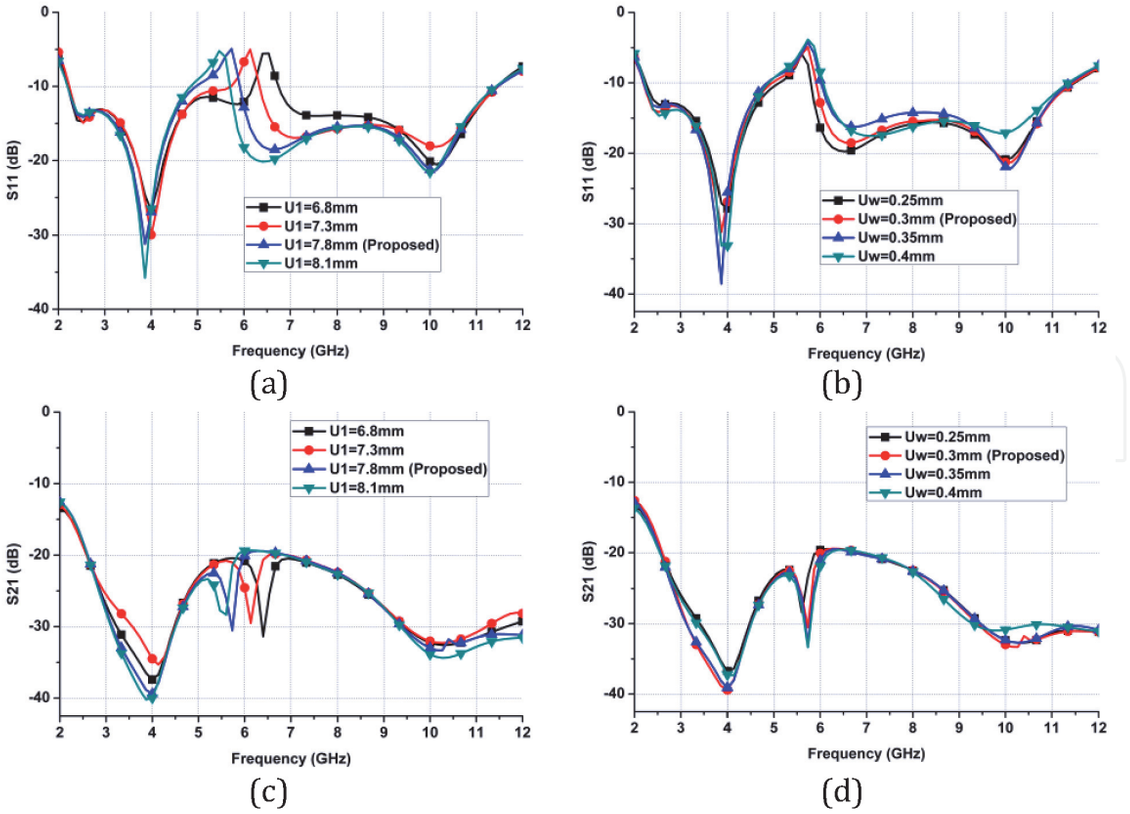

Figure 11.
S11-parameter for (a) various slot lengths, (b) various slot widths; and S21 for (c) various slot lengths, (d) various slot widths.

mm to 0.4 mm, the notch bandwidth is increasing from (5.2–5.7) GHz to (4.94–6.1) GHz with notch center frequency f_N at 5.7 GHz. The slot width U_W of 0.3 mm is chosen in this proposed design to get the desired band notch from 5 to 5.9 GHz. **Figure 11(c)** and **(d)** shows the effects of inverted U-slot resonator on the S_{21} of the MIMO antenna for various slot lengths and widths. Also, it is observed that variation in the slot length U_1 and width U_W has a negligible effect on the mutual coupling of MIMO antenna.

2.3 Results and discussion

The proposed antenna offers good impedance bandwidth ($|S_{11}| < -10$ dB) from 2.2 to 11.4 GHz with band notch at 5–5.9 GHz as demonstrated in **Figure 12(a)**. Hence, the frequency interference from WLAN band can be effectively suppressed by the proposed UWB MIMO antenna. And, from **Figure 12(b)**, it is found that the simulated and measured mutual coupling (S_{21}) value is about −20 dB in the operating band except at few frequencies around 6.2 and 7.2 GHz (−18 dB) demonstrating good isolation between the ports. At 6.2 and 7.2 GHz the S_{21} is −16 dB. From **Figure 12(c)**, the antenna has good 2:1 VSWR from 2.2 to 11.4 GHz excluding at notch-band, i.e. from 5.0 to 5.9 GHz. It is observed that the VSWR of about 3.5 at 5.7 GHz. The summary of simulated and mesured results presented in **Figure 12** are provided in **Table 3**. The simulated and measured radiation patterns of the proposed antenna on the *E*-plane and *H*-plane at 3.8, 6.5, and 10 GHz when port 1 is excited and port 2 is terminated with 50-ohm load, and vice-versa are shown in **Figure 13(a)** and **(b)**. Good agreement between the simulated and measure 2-D radiation patterns is observed. At 3.8 and 6.5 GHz frequencies, PM1 and PM2 have quite omnidirectional radiation patterns in H-planes, i.e. the *XZ* plane and the *YZ* plane, respectively. However, at 10 GHz because of the higher-order resonances,

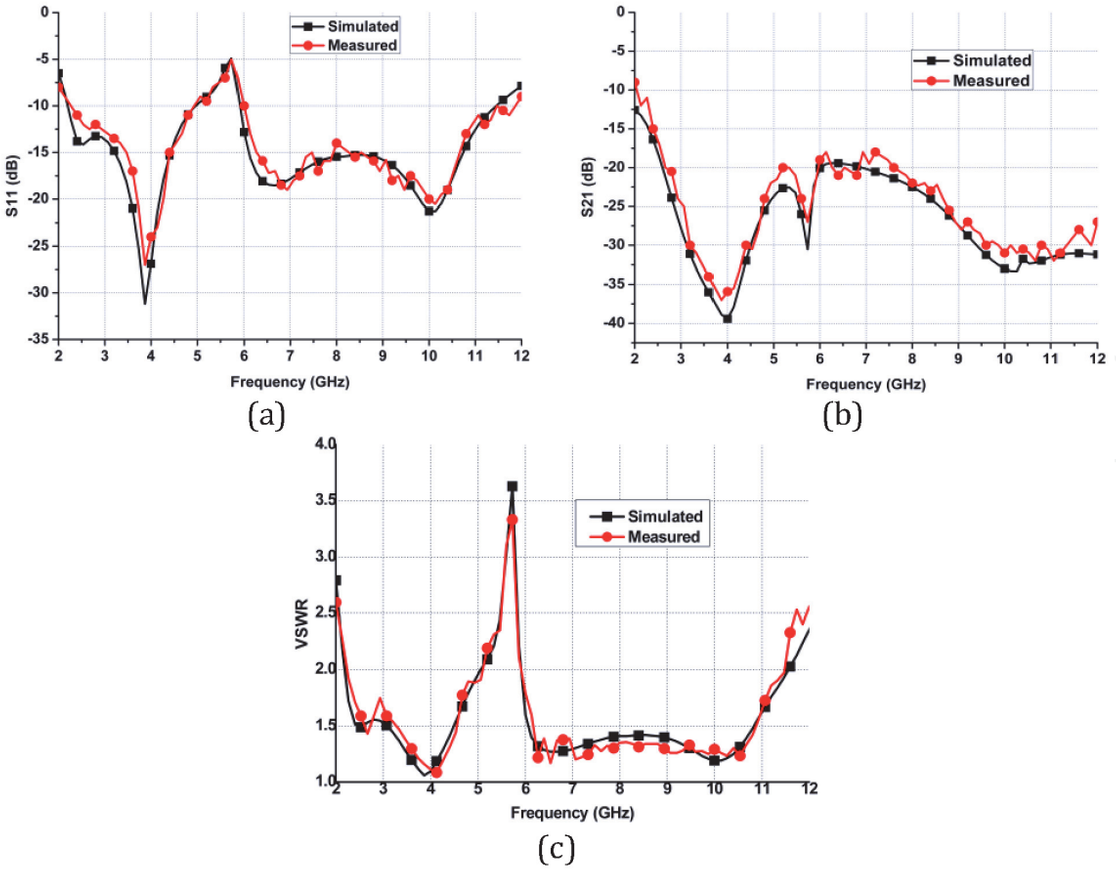

Figure 12.
The simulated and measured results: (a) S11-parameter, (b) S21-parameter and (c) VSWR

Result	Bandwidth ($S_{11} < -10$ dB)	Mutual coupling (S_{21})	VSWR at notch band	Notch band
Simulated	2.2–11.4 GHz	<−20 dB	3.6	5–5.9 GHz
Measured	2.3–11.7 GHz	<−18 dB	3.4	5–6 GHz

Table 3.
The summary of simulated and measured results presented in ***Figure 12****.*

the radiation patterns in the *H*-planes are less omnidirectional. And, at 6.5 and 10 GHz, PM1 and PM2 have the dumbbell-shaped or bidirectional patterns in the *E*-planes, i.e. the *YZ* plane and the *XZ* plane, respectively. However, at 3.8 GHz, PM1 and PM2 do not have the "dumb-bell" shaped patterns in the *E*-planes, because, the strip on the ground plane changes the current distributions. It can be seen from **Figure 13** that the proposed antenna provides omnidirectional radiations in *H*-plane which is essential for portable wireless devices to receive the signals from all directions. And, it is also found that *H*-plane patterns of port 1 and port 2 are nearly mirror images demonstrating the good pattern diversity. The simulated and measured peak gain of the proposed design is plotted in **Figure 14(a)**. The peak gain of 2.4 to 7.5 dBi in the operating band is observed excepting at the notch band. At the notch band, the measured peak gain falls to −2.2 dBi. **Figure 14(b)** shows the simulated and measured radiation efficiency plot of the proposed antenna. The radiation efficiency of above 90% is found across the UWB band excluding at 5–5.9 GHz notch band. At notch band, the efficiency drops to 12%. It is evident from **Figure 14(a)** and **(b)** that the proposed antenna can avoid the frequency interference from WLAN band more efficiently.

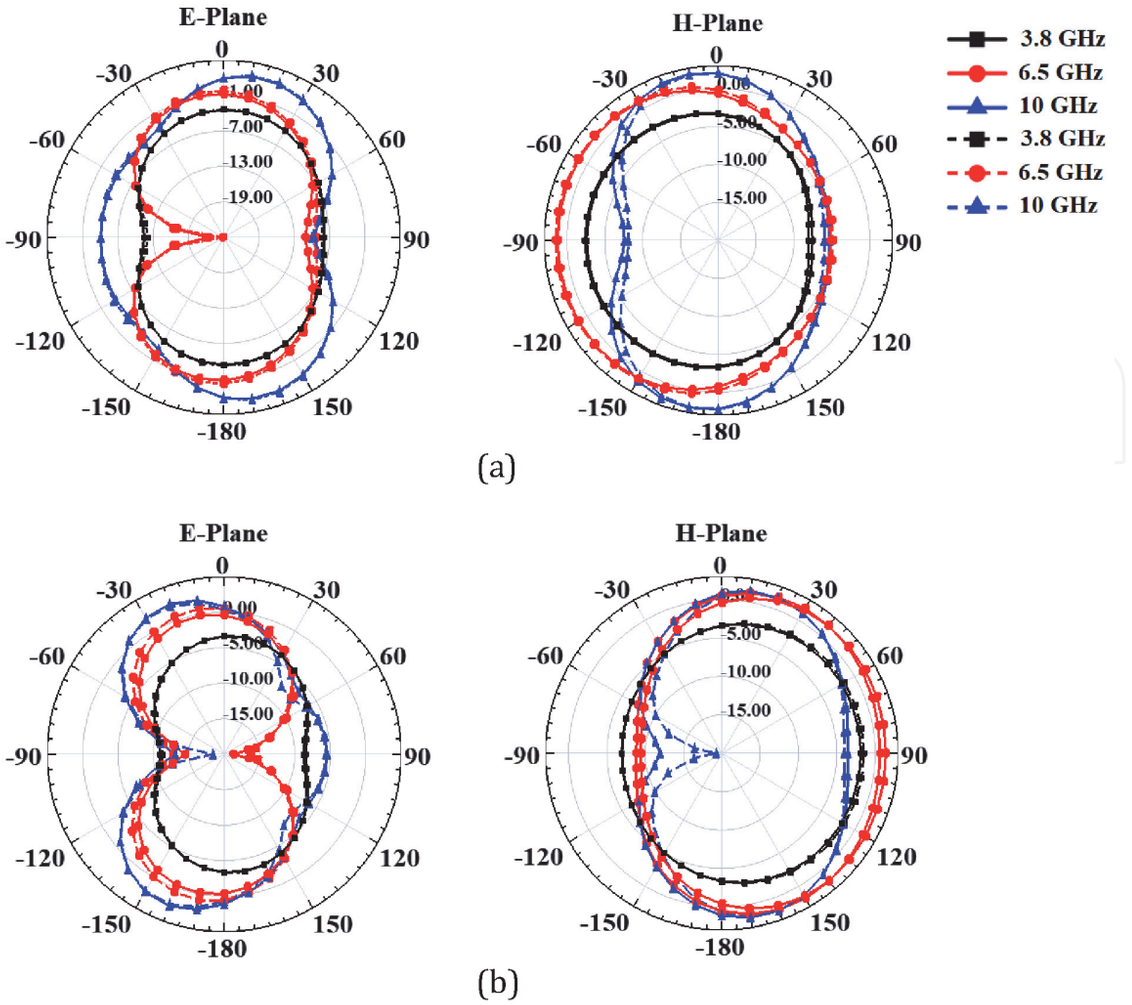

Figure 13.
Simulated (solid line) and measured (dashed line) radiation patterns. (a) simulated and measured when port 1 excited. (b) Simulated and measured when port 2 excited.

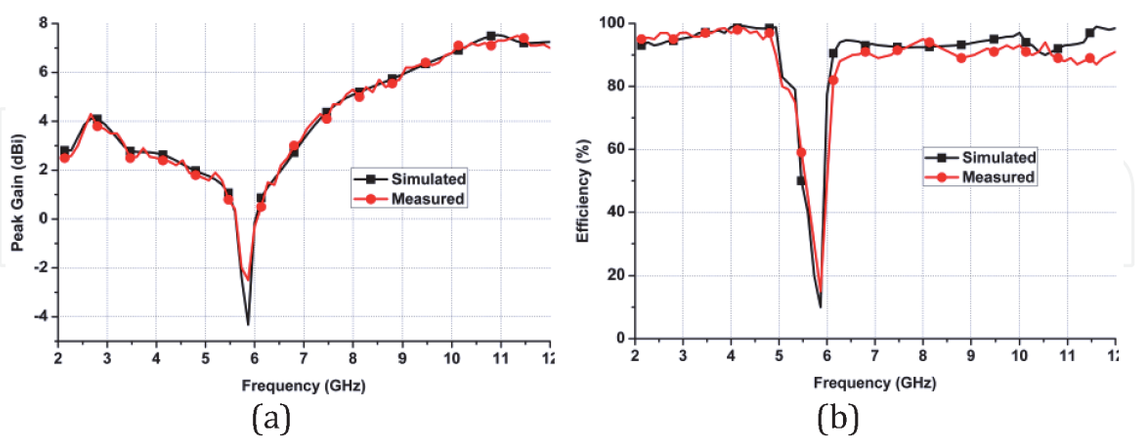

Figure 14.
Simulated and measured (a) peak gain, (b) radiation efficiency.

Along with the radiation patterns, envelope correlation coefficient (ECC) is also an important parameter to study the MIMO antenna diversity and is calculated using *S*-parameters with the equation (7) of a two-port MIMO antenna system reported by Blanch et al. [32]. The envelop correlation coefficient (ECC) measures the similarity between the antenna radiation patterns and is very useful to estimate the performance of MIMO antenna. The lower the ECC value means the lesser is the

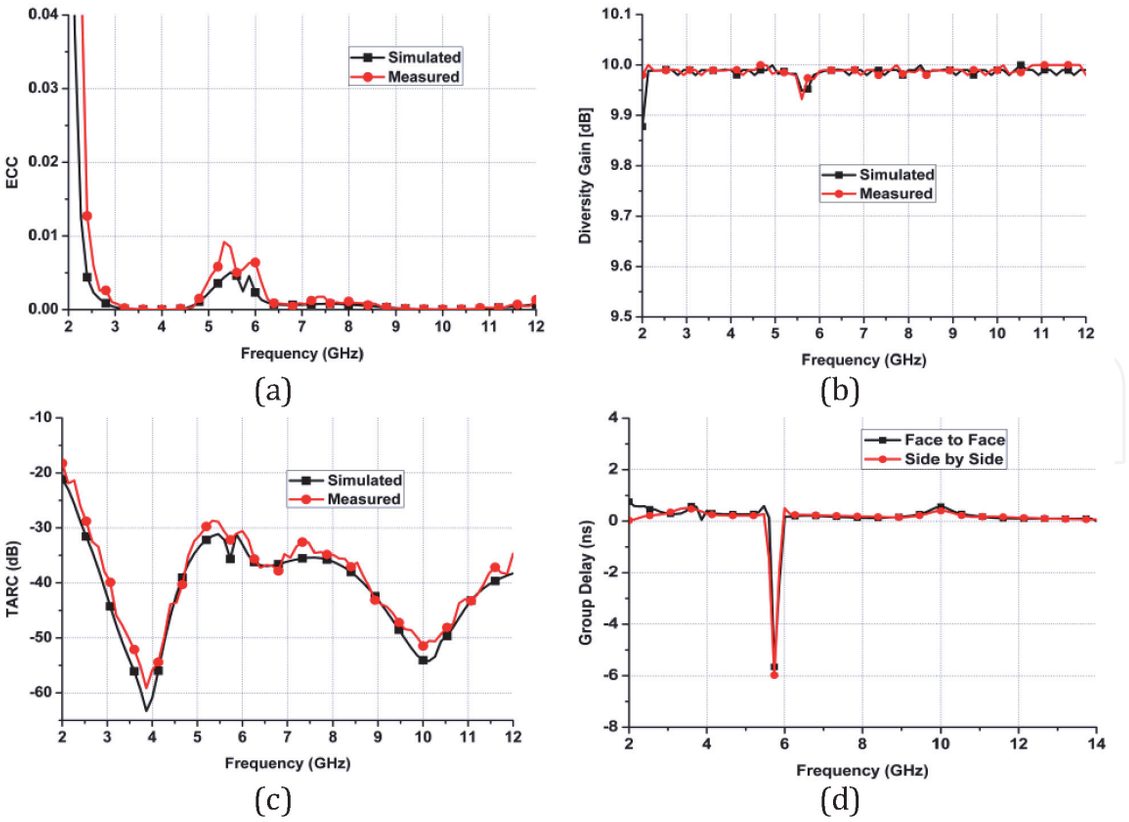

Figure 15.
(a) Simulated and measured ECC, (b) Simulated and measured diversity gain, (c) Simulated and measured TARC, (d) Group delay of the proposed antenna.

overlapping between the two radiation patterns. For MIMO antenna system to ensure the diversity performance as good, the ECC with value below 0.5 is adopted in most the cases. **Figure 15(a)** shows the simulated and measured ECC of the proposed antenna. The simulated ECC is about 0.005 and measured ECC is below 0.008 from 2.2 to 11.4 GHz.

$$ECC = \frac{\left|S_{11}^{*}S_{12} + S_{21}^{*}S_{22}\right|^{2}}{\left(1 - \left(\left|S_{11}\right|^{2} + \left|S_{21}\right|^{2}\right)\right)\left(1 - \left(\left|S_{22}\right|^{2} + \left|S_{12}\right|^{2}\right)\right)}, \tag{7}$$

The diversity gain (DG) and total active reflection coefficient (TARC) are also essential parameters to study the MIMO antenna diversity performance. The diversity gain and total active reflection coefficient of the proposed antennas can be estimated by using the equations (8) and (9) [33] as follows:

$$DG = 10\sqrt{1 - ECC^{2}} \tag{8}$$

$$TARC = \sqrt{\frac{\left(S_{11} + S_{12}\right)^{2} + \left(S_{21} + S_{22}\right)^{2}}{2}} \tag{9}$$

The simulated and measured diversity gain plots are given in **Figure 15(b)**. The diversity gain of >9.95 dB is found in the UWB band. And, **Figure 15(c)** shows the simulated and measured TARC. It is observed that the TARC of less than −28 dB is obtained in the whole UWB band. The group delay of the proposed antenna is measured in face to face and side by side situations with the space of 30 cm is shown in **Figure 15(d)**. The group delay is almost uniform and is below 1 ns in the

complete working band except at stopband. At the notch band i.e. at 5.7 GHz, the group delay of 5.8 ns in the face to face orientation and 6 ns in the side by side orientation ensures that the proposed antenna can transmit the UWB signal with minimum distortion. It is observed from the above results that there is good agreement between the simulated and measured *S*-parameters except for some deviations due to fabrication and soldering imperfections, losses in dielectrics and conductors, effects of SMA connector, and measurement tolerances.

3. Conclusion

To mitigate the frequency interference from narrowband system like WLAN, a compact planar UWB antenna with single band-notched characteristics for portable wireless devices applications is discussed in this chapter. In this design, the monopoles are arranged perpendicularly to reduce to mutual coupling. A rectangular strip is extended from the ground plane to improve the impedance matching characteristics and to reduce the mutual coupling further or enhance the isolation. An inverted U-shaped slot is used on the feed line to realize the band-notch filtering function for suppressing the frequency interference from 5 to 5.9 GHz WLAN band. For validating the simulation results, all the proposed antennas have been fabricated and tested using the Agilent N5224A PNA, Anritsu MS2037C vector network analyzer and an anechoic chamber. The measured results of all the proposed antenna are well agreed with simulated results. The measured and simulated results show that the proposed antenna offer good impedance bandwidth of $S_{11} \leq -10$ dB in whole UWB band (3.1–10.6 GHz) except at the designed notch bands while giving less mutual coupling (S_{21}) of lower than −20 dB in the entire UWB band. The low envelope correlation coefficient, nearly constant gain, stable radiation patterns, more directive gain, TARC and less group delay, demonstrate that the proposed MIMO antenna is an appropriate choice for portable wireless UWB systems.

Acknowledgements

Authors would like to express their gratitude towards University College of Engineering & Technology, Acharya Nagarjuna University, Guntur and management of Koneru Lakshmaiah Education Foundation, Guntur for their continuous support and encouragement during this work. Further, Dr. J. Chandrasekhar Rao and Dr. N. Venkateswara Rao would like to acknowledge with thanks DST through FIST grant SR/FST/ETI-316/2012, ECR/2016/000569 and Dr. B.T.P. Madhav, Prof. of ECE, KLEF for providing measurement facility in LCRC lab. I would like to thank Mr. P. Ramakoti Reddy, Electro Circuit Systems, Hyderabad, Mr. K. Vijaya Saradhi Reddy, Excel Radio Frequency Technologies, Hyderabad and Mr. Krishna Prasad, Scientist-ECIL, Hyderabad for their help in the fabrication and measurements of the prototype developed in this work.

Author details

Chandrasekhar Rao Jetti* and Venkateswara Rao Nandanavanam
Bapatla Engineering College, Bapatla, Andhra Pradesh, India

*Address all correspondence to: jettychandu@gmail.com

References

[1] Federal Communications Commission (FCC), Revision of Part 15 of the Commission's Rules Regarding Ultra-Wideband Transmission Systems First Rep. and Order, ET Docket 98-153, FCC 02-48, Adopted: Feb. 2002; Released, Apr. 2002.

[2] Kaiser T, Zheng F, Dimitrov E. An overview of ultra-wide-band systems with MIMO. Proceedings of the IEEE. 2009 Feb 27;97(2):285-312.

[3] Mabrouk IB, Talbi L, Nedil M, Hettak K. MIMO-UWB channel characterization within an underground mine gallery. IEEE Transactions on Antennas and Propagation. 2012 Jul 10; 60(10):4866-74.

[4] Tran VP, Sibille A. Spatial multiplexing in UWB MIMO communications. Electronics letters. 2006 Aug 3;42(16):1.

[5] Zheng L, Tse DN. Diversity and multiplexing: A fundamental tradeoff in multiple-antenna channels. IEEE Transactions on information theory. 2003 May 7;49(5):1073-96.

[6] Liu L, Cheung SW, Yuk TI. Compact MIMO antenna for portable devices in UWB applications. IEEE Transactions on antennas and propagation. 2013 May 15;61(8):4257-64.

[7] Zhang S, Ying Z, Xiong J, He S. Ultrawideband MIMO/diversity antennas with a tree-like structure to enhance wideband isolation. IEEE Antennas and Wireless Propagation Letters. 2009 Nov 24;8:1279-82.

[8] Luo CM, Hong JS, Zhong LL. Isolation enhancement of a very compact UWB-MIMO slot antenna with two defected ground structures. IEEE Antennas and Wireless Propagation Letters. 2015 Apr 15;14: 1766-9.

[9] Tao J, Feng Q. Compact ultrawideband MIMO antenna with half-slot structure. IEEE Antennas and wireless Propagation letters. 2016 Aug 30;16:792-5.

[10] Gallo M, Antonino-Daviu E, Ferrando-Bataller M, Bozzetti M, Molina-Garcia-Pardo JM, Juan-Llacer L. A broadband pattern diversity annular slot antenna. IEEE Transactions on Antennas and propagation. 2011 Dec 20; 60(3):1596-600.

[11] Rao JC, Rao NV. CPW-fed compact ultra wideband MIMO antenna for portable devices. Indian Journal of Science and Technology. 2016 May;9 (17):1-9.

[12] Bassi M, Caruso M, Khan MS, Bevilacqua A, Capobianco AD, Neviani A. An integrated microwave imaging radar with planar antennas for breast cancer detection. IEEE Transactions on microwave theory and techniques. 2013 Feb 26;61(5): 2108-18.

[13] Capobianco AD, Khan MS, Caruso M, Bevilacqua A. 3–18 GHz compact planar antenna for short-range radar imaging. Electronics letters. 2014 Jun 27;50(14):1016-8.

[14] Zhang S, Pedersen GF. Mutual coupling reduction for UWB MIMO antennas with a wideband neutralization line. IEEE antennas and wireless propagation letters. 2015 May 21;15:166-9.

[15] Li H, Liu J, Wang Z, Yin YZ. Compact 1× 2 and 2× 2 MIMO antennas with enhanced isolation for ultrawideband application. Progress In Electromagnetics Research. 2017;71: 41-9.

[16] Kerkhoff A, Ling H. Design of a planar monopole antenna for use with

ultra-wideband (UWB) having a band-notched characteristic. InIEEE Antennas and Propagation Society International Symposium. Digest. Held in conjunction with: USNC/CNC/URSI North American Radio Sci. Meeting (Cat. No. 03CH37450) 2003 Jun 22 (Vol. 1, pp. 830-833). IEEE.

[17] Weng YF, Cheung SW, Yuk TI, Liu L. Creating band-notched characteristics for compact UWB monopole antennas. InUltra Wideband-Current Status and Future Trends 2012 Oct 3. IntechOpen.

[18] Liu L. Compact planar UWB antennas for wireless device applications. HKU Theses Online (HKUTO). 2014.

[19] Zheng ZA, Chu QX, Tu ZH. Compact Band-Rejected Ultrawideband Slot Antennas Inserting With λ/2 and λ/4 Resonators. IEEE Transactions on Antennas and Propagation. 2011 Feb;59 (2):390-7.

[20] Weng YF, Cheung SW, Yuk TI. Compact ultra-wideband antennas with single band-notched characteristic using simple ground stubs. Microwave and Optical Technology Letters. 2011 Mar;53 (3):523-9.

[21] Lee JM, Kim KB, Ryu HK, Woo JM. A compact ultrawideband MIMO antenna with WLAN band-rejected operation for mobile devices. IEEE Antennas and wireless propagation letters. 2012 Aug 21;11:990-3.

[22] Sayidmarie KH, Najm TA. Performance evaluation of band notch techniques for printed dual band monopole antennas. International Journal of Electromagnetics and Applications. 2013;3(4):70-80.

[23] Majeed AH, Abdullah AS, Sayidmarie KH, Abd-Alhameed RA, Elmegri F, Noras JM. Compact dielectric resonator antenna with band-notched characteristics for ultra-wideband applications. Progress In Electromagnetics Research. 2015;57: 137-48.

[24] Gao P, He S, Wei X, Xu Z, Wang N, Zheng Y. Compact printed UWB diversity slot antenna with 5.5-GHz band-notched characteristics. IEEE Antennas and Wireless Propagation Letters. 2014 Feb 14;13:376-9.

[25] Khan MS, Capobianco AD, Naqvi A, Shafique MF, Ijaz B, Braaten BD. Compact planar UWB MIMO antenna with on-demand WLAN rejection. Electronics Letters. 2015 Jun 3;51(13): 963-4.

[26] Liu L, Cheung SW, Yuk TI. Compact MIMO antenna for portable UWB applications with band-notched characteristic. IEEE Transactions on Antennas and Propagation. 2015 Feb 24; 63(5):1917-24.

[27] Sipal D, Abegaonkar MP, Koul SK. Compact band-notched UWB antenna for MIMO applications in portable wireless devices. Microwave and Optical Technology Letters. 2016 Jun;58(6): 1390-4.

[28] Tao J, Feng QY. Compact isolation-enhanced UWB MIMO antenna with band-notch character. Journal of ElEctromagnEtic WavEs and applications. 2016 Nov 1;30(16): 2206-14.

[29] Liu Z, Wu X, Zhang Y, Ye P, Ding Z, Hu C. Very compact 5.5 GHz band-notched UWB-MIMO antennas with high isolation. Progress In Electromagnetics Research. 2017;76: 109-18.

[30] Tripathi S, Mohan A, Yadav SK. A compact MIMO/diversity antenna with WLAN band-notch characteristics for portable UWB applications. Progress In Electromagnetics Research. 2017;77: 29-38.

[31] Jetti CR, Nandanavanam VR. Compact MIMO antenna with WLAN band-notch characteristics for portable UWB systems. Progress In Electromagnetics Research. 2018;88: 1-12.

[32] Blanch S, Romeu J, Corbella I. Exact representation of antenna system diversity performance from input parameter description. Electronics letters. 2003 May 1;39(9):705-7.

[33] Najam AI, Duroc Y, Tedjini S. Multiple-input multiple-output antennas for ultra wideband communications. IntechOpen. 2012 Oct 1;10:209-36.